Probing the Solid Earth with Cosmic-Ray Muons: From Volcanoes to Crust-Mantle Transition Zones

László Oláh[1,10]; László Tercsi[1]; Dezső Varga[1,10]; Haruhisa Nakamichi[2]; Hiroyuki K. M. Tanaka[3,10]; Seiki Kubo[4]; Sinya Yoshida[4]; Kazumichi Iwata[4]; Junichi Akanuma[5]; Masafumi Kaneko[5]; Hisashi Watanabe[5]; Yuki Kusano[6]; Tomoaki Morishita[7,8]; Susumu Umino[8]; Said Mohammed Almusharafi[9]; Nasser Saif Said Al-Maawali[9]; Ibrahim Awadh Mohammed Al Sawafi[9]

1 Institute for Particle and Nuclear Physics, HUN-REN Wigner RCP, Budapest, Hungary
2 Disaster Prevention Research Institute, Kyoto University, Kyoto, Japan
3 Earthquake Research Institute, The University of Tokyo, Tokyo, Japan
4 Unzen Sabo Management Center, Kyushu Regional Development Bureau, MLIT, Nagasaki, Japan
5 Sabo Frontier Foundation (SFF), Tokyo, Japan
6 Geological Survey of Japan, Tsukuba, Japan
7 Volcanoes and Earth's Interior Research Center, Research Institute for Marine Geodynamics, Japan Agency for Marine-Earth Science and Technology, Yokosuka, Japan
8 College of Science and Engineering, Kanazawa University, Kanazawa, Japan
9 Ministry of Energy and Minerals, Muscat, Sultanate of Oman
10 International Virtual Muography Institute, Global

3 June 2026

PROGRAM FINANCED FROM THE NRDI FUND

Outline

I. Magma migration Inferred from Joint Muon and Ground Deformation Monitoring

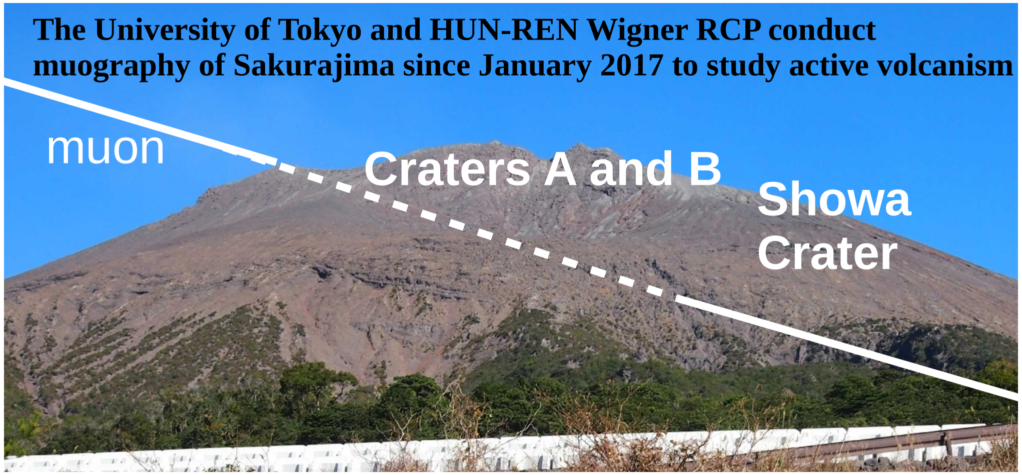

D. Varga et al. Advances in High Energy Physics, 2016, 1962317 https://doi.org/10.1155/2016/1962317

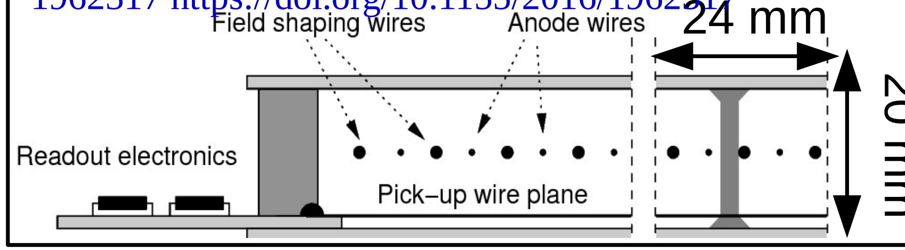

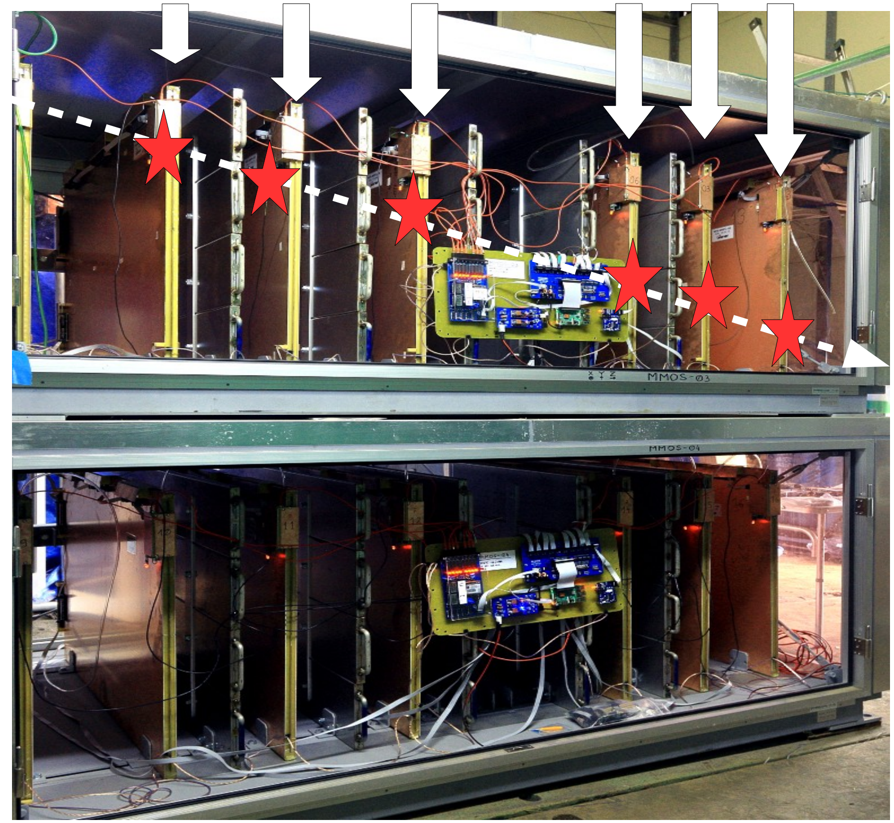

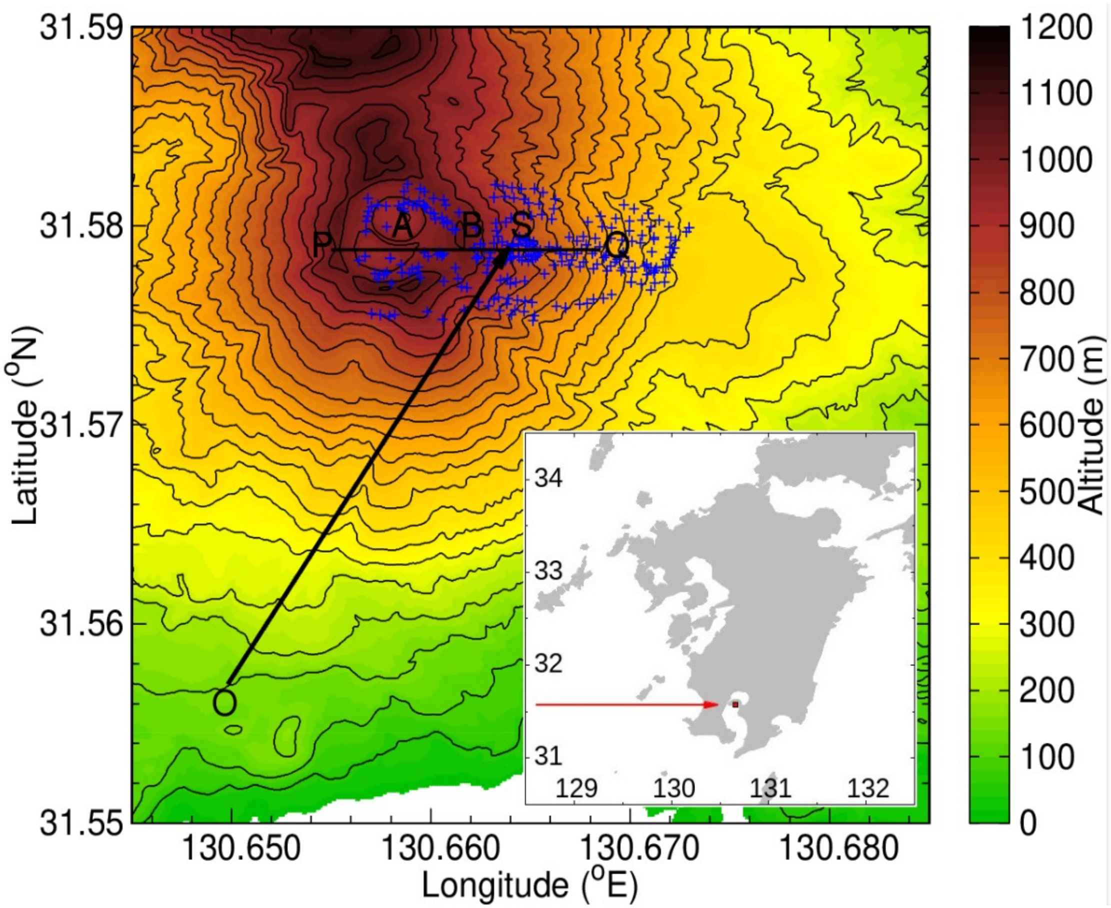

Mugrapic Observation Instrument WO2017187308
https://patentscope2.wipo.int/search/en/detail.jsf?docId=WO2017187308
L. Oláh et al. Scientific Reports, 8, 3207, 2018,
https://doi.org/10.1038/s41598-018-21423-9
D. Varga et al. Nucl. Instrum. Meth. A 958, 162236, 2020
https://doi.org/10.1016/j.nima.2019.05.077

I. Magma migration Inferred from Joint Muon and Ground Deformation Monitoring

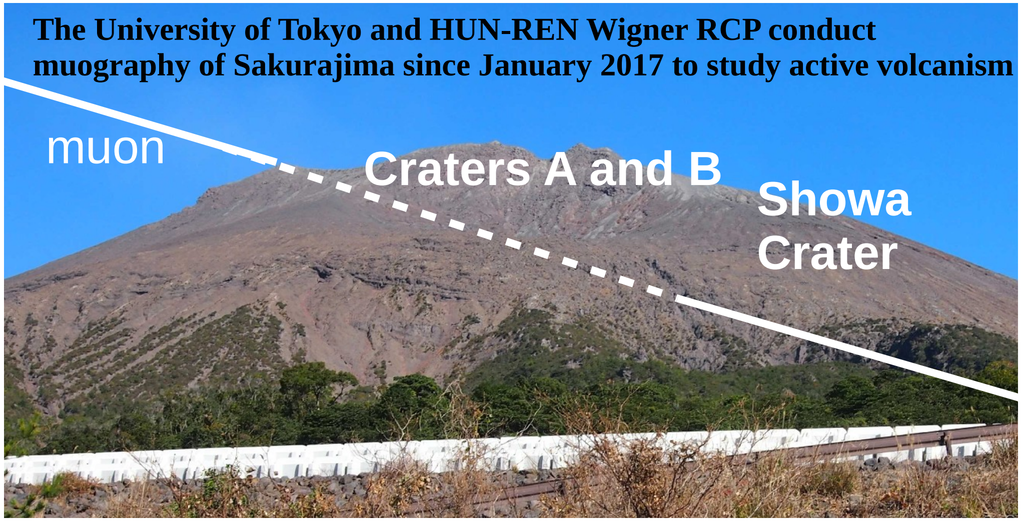

- Density images were recorded from 1 Oct. 2018 to 29 Feb. 2024
- 6-month moving average values of densities were calculated beneath the Minamidake A, B and Showa craters

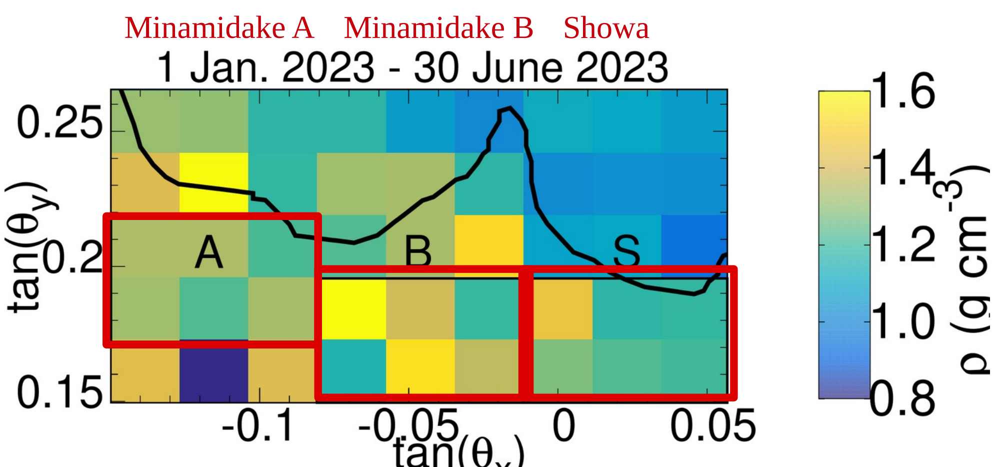

- **Masses were calculated for trapezoid volumes:**

$$m = N\,\rho_{mean} T_{mean}[D^2\Delta^2 + (D + T_{mean})^2\Delta^2 + D\,(D + T_{mean})\,\Delta^2]/\,3$$

D. Varga et al. Advances in High Energy Physics, 2016, 1962317 https://doi.org/10.1155/2016/1962317

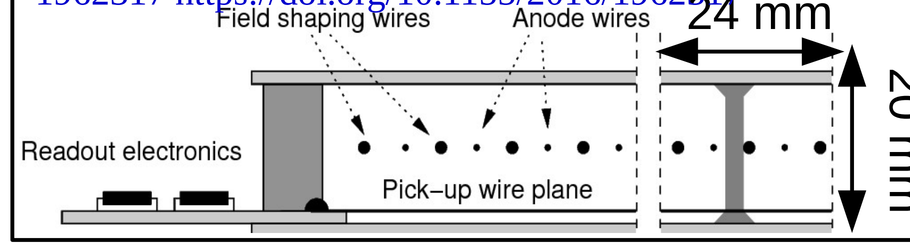

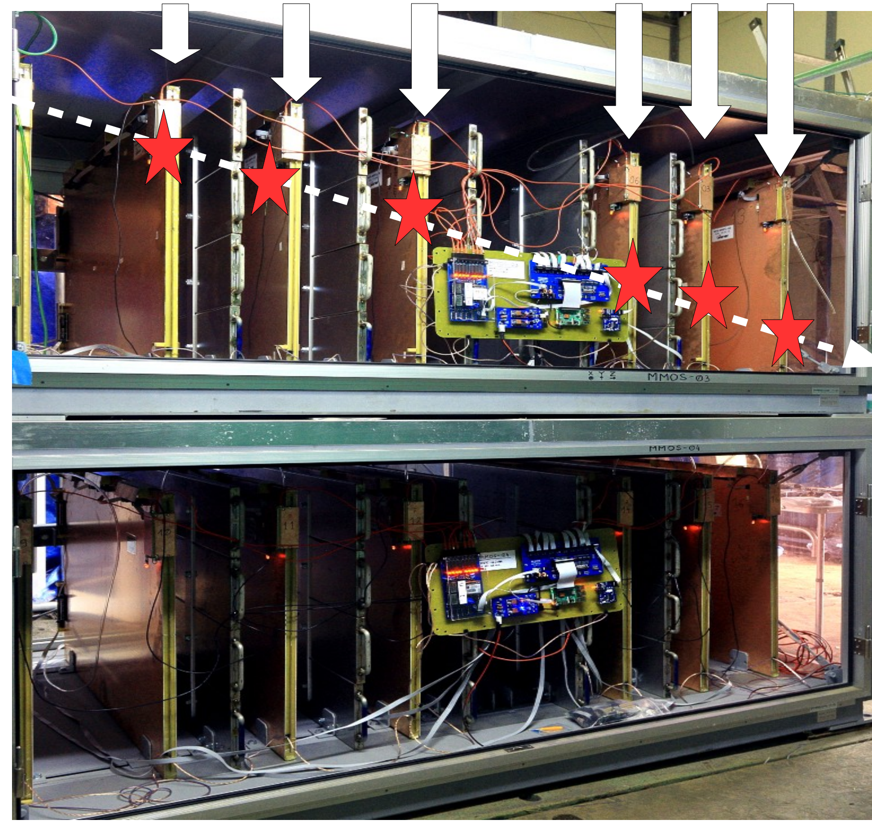

Muograpic Observation Instrument WO2017187308
https://patentscope2.wipo.int/search/en/detail.jsf?docId=WO2017187308
L. Oláh et al. Scientific Reports, 8, 3207, 2018, https://doi.org/10.1038/s41598-018-21423-9
D. Varga et al. Nucl. Instrum. Meth. A 958, 162236, 2020 https://doi.org/10.1016/j.nima.2019.05.077

Mogi and Yang Modeling of Ground Surface Deformations Measured by InSAR

Vertical displacement around the active crater of Sakurajima was determined relative to the ground level measured on 31 October 2018 by NEC using the Phased Array type C-band Synthetic Aperture Radar images acquired by Sentinel-1 **with a periodic time of 12 days.**

- Comparison of modeled and measured (above altitude of 700 m) vertical uplifts enables us to determine volume change and spatial coordinates of pressure source
- **Parameter estimation procedure based on grid searching** via minimizing the square of relative difference between the measured and modeled vertical uplifts of ground surface as a function of the radial distance

(a) Mogi: $U_v = 3\,\Delta V\, D \;/\; [\,4\pi\,(R^2 + D^2)^{3/2}\,]$

(b) Yang: $U_v = \Delta P abc \;/\; [\,\mu\,(R^2 + D^2)^{3/2}\,]$

where

μ is the shear modulus of medium.

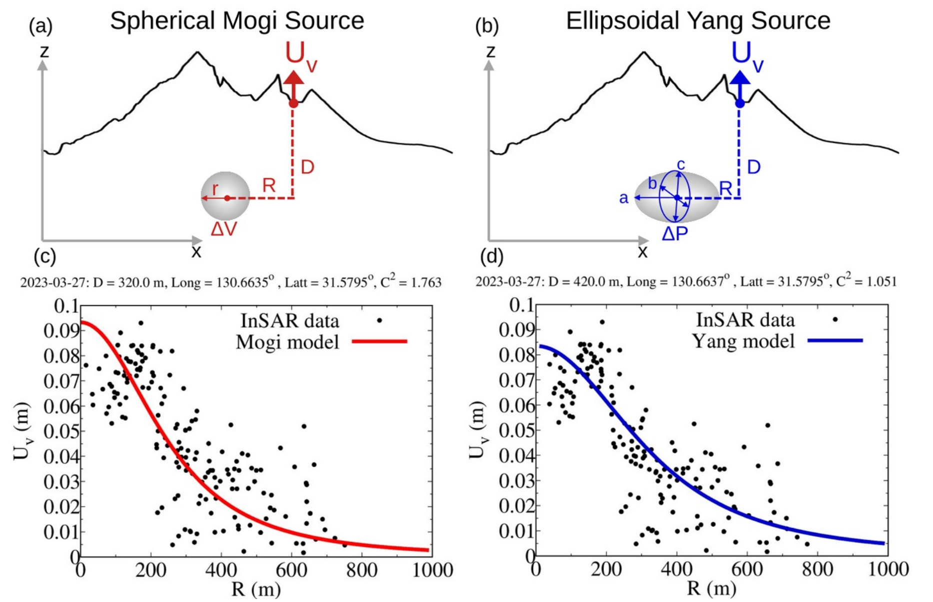

Comparison of Mogi and Yang source modeling:

(a) Source movement is negligible in N-S dierection,

(b) Source movement of a few hundred meters in W-E direction,

(c) Source depth decreased over time. A slight shift is visible between the two depths.

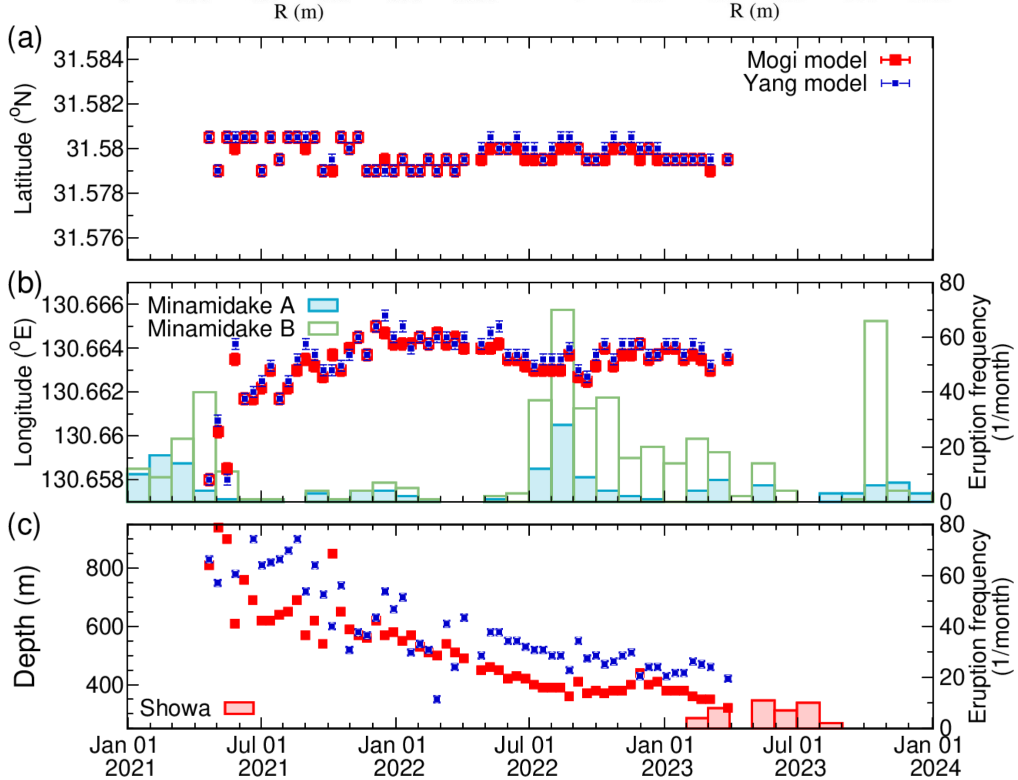

Magma migration towards east in 2021

Source modelling: The deformation source moved towards east beneath the active craters at a depth of 600-700 m.

Muography: *the mass decreased beneath* Mindamidake A and Minamidake B craters, and increased beneath the Showa crater.

Eruption frequency: Shifted from crater Minamidake A to crater Minamidake B.

→ **(1) Deep horizontal magma channel at 600-700 m beneath the active craters that feeds the Minamidake.**

Magnetotelluric measurements has already indicated similar horizontal structure at similar depths.
Aizawa, et al. (2011) J Volcanol Geotherm Res199:165-175. https://doi.org/10.1016/j.jvolgeores.2010.11.003

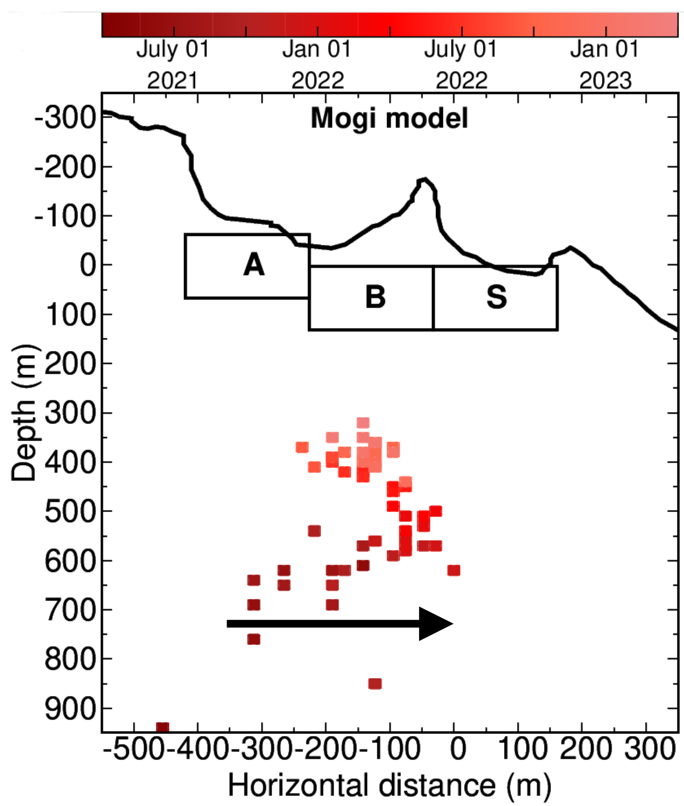

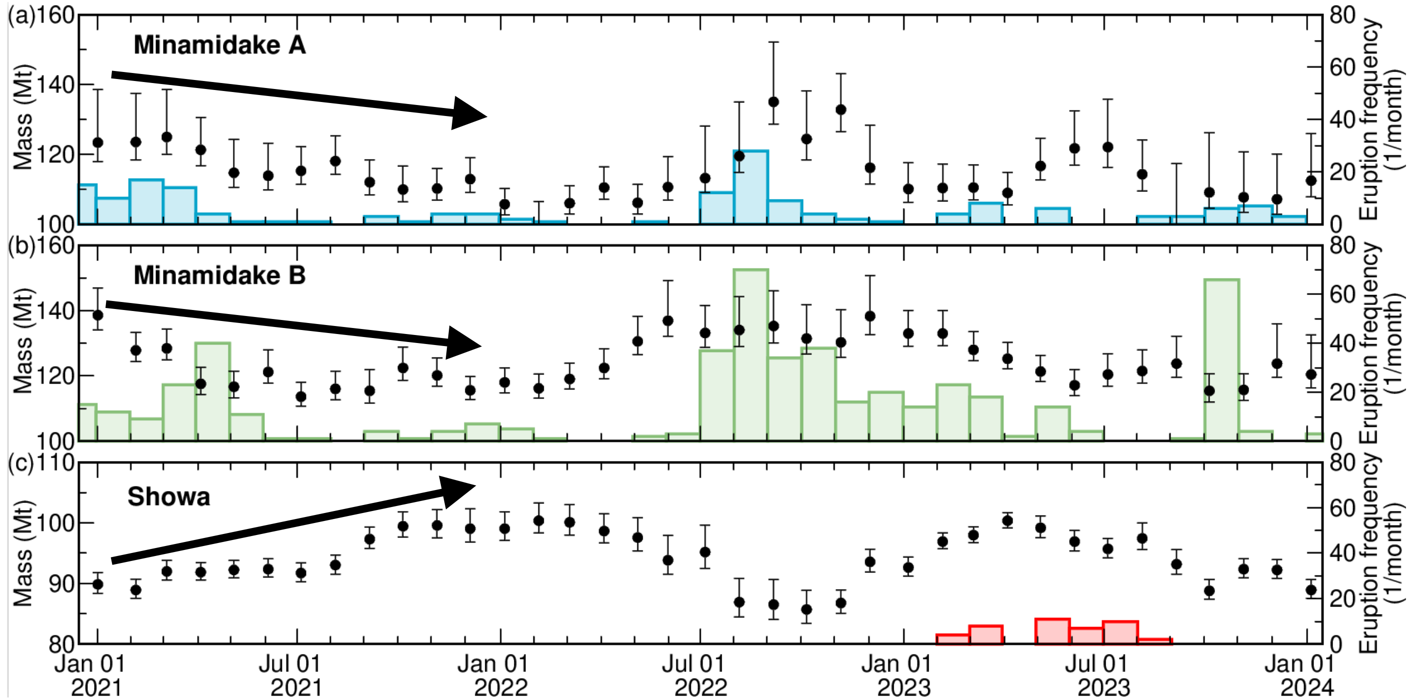

L. Oláh, et al. Magma migration beneath the active craters of Sakurajima volcano before the 2023 eruption of Showa crater inferred from ground deformation and muon monitoring. Earth Planets Space 77, 196 (2025). https://doi.org/10.1186/s40623-025-02325-3

Magma rising before the eruption 2023 of Showa crater

Source modelling*:* the source of ground deformation rised about 350 m beneath the active craters

Muography*:* the mass increased beneath the Showa crater.

Eruption frequency*:* The Showa crater started to erupt in early 2023. The Minamidake craters remained actice.

→ **(2) Shallow magma reservoir that feeds all craters with magma**

Magma head rising was also observed earlier by absolute gravimetry
(Okubo, et al. (2013) Bull Volcanol Soc Japan 58:153-162. https://doi.org/10.18940/kazan.58.1_153).
Active seismic experiments and rock sample analysis also suggest the presence of a shallow magma reservoir
(Nishimura, et al. (2024). Bull Volcanol 86:27. https://doi.org/10.1007/s00445-024-01722-y).

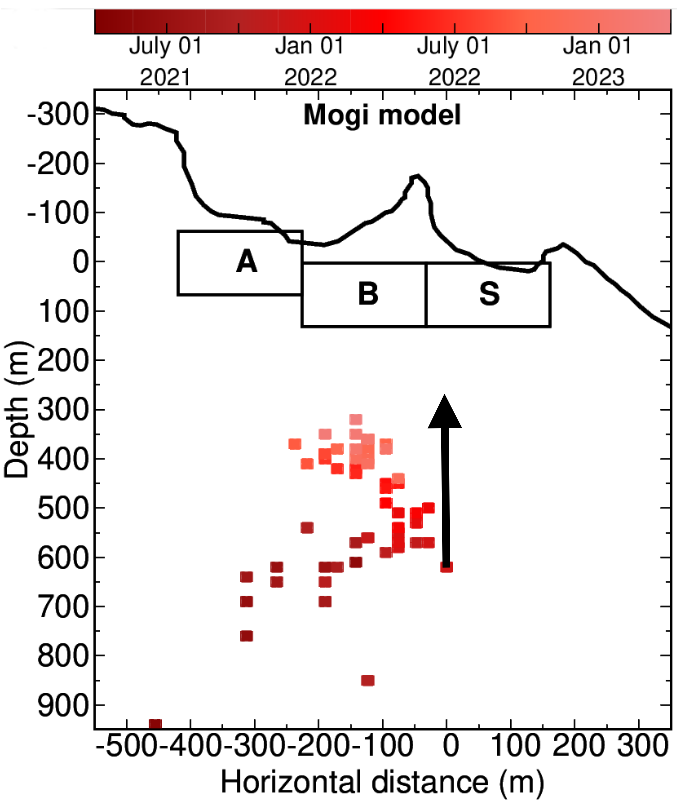

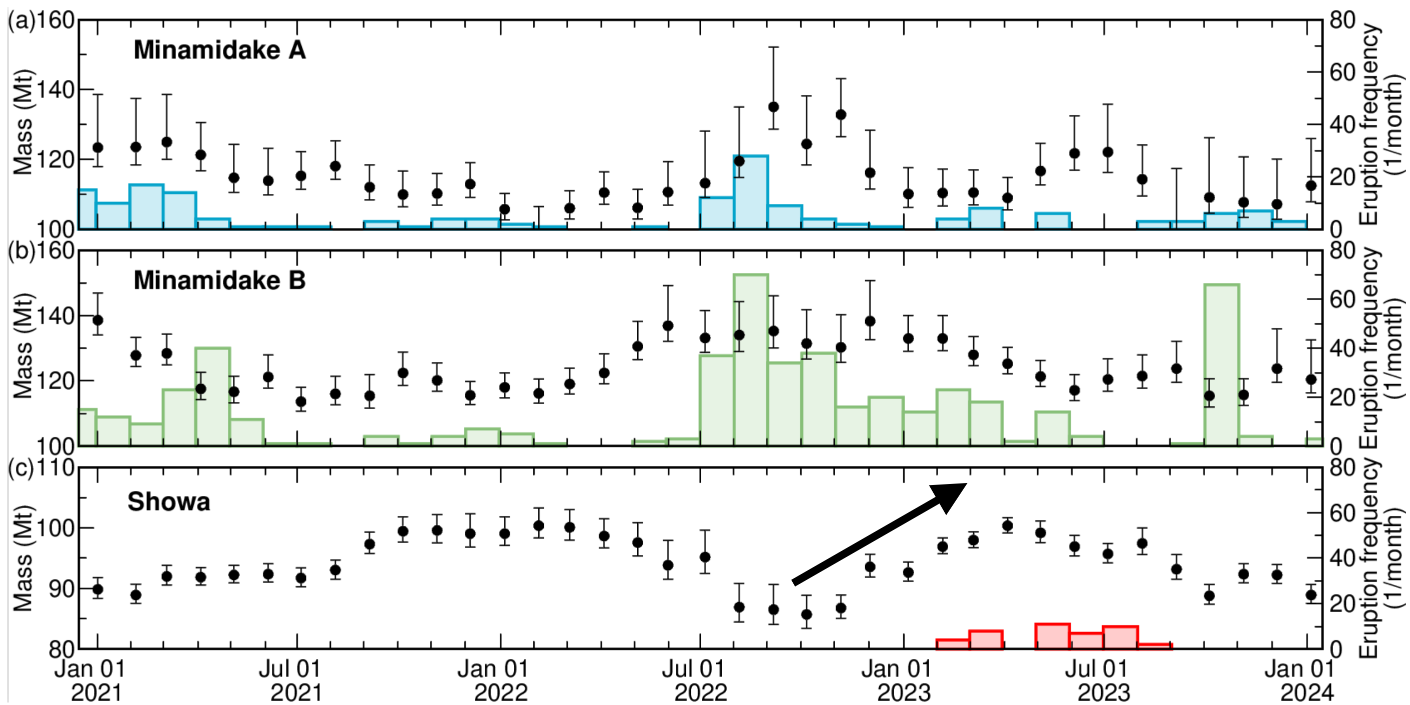

L. Oláh, et al. Magma migration beneath the active craters of Sakurajima volcano before the 2023 eruption of Showa crater inferred from ground deformation and muon monitoring. Earth Planets Space 77, 196 (2025). https://doi.org/10.1186/s40623-025-02325-3

III. Structural Characterization of Mount Unzen

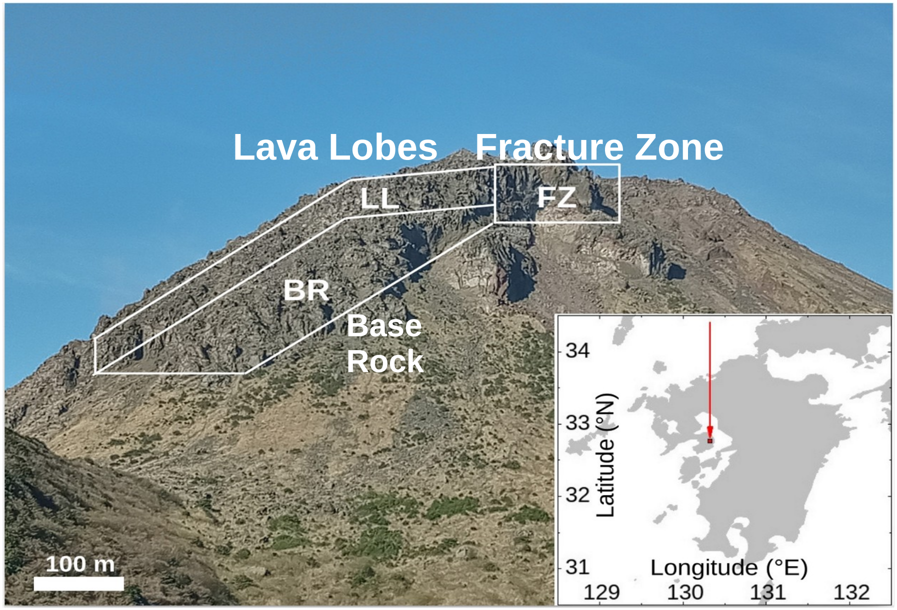

Lava lobes deposited on the summit of Mount Unzen during the eruption of 1990-1995.

Nakada, S., Shimizu, H. & Ohta, K., 1999. J. Volc. Geotherm. Res., 89, 1–22
https://doi.org/10.1016/S0377-0273(98)00118-8

Destabilization of lava lobes can generate debris avalanches with catastrophic impacts.

MOS was installed at a longitude of 130.322515 E◦ and a latitude of 32.769151 N◦ at an altitude of 576 m above sea level at a distance of about 2000 m in a northeast direction from the Fugendake peak.

The MOS was oriented to the azimuthal direction of 236.5◦ from north and tilted up 11.5◦ from the horizontal direction.

The data collection was performed for **203 days between March 28 and December 14 in 2024.**

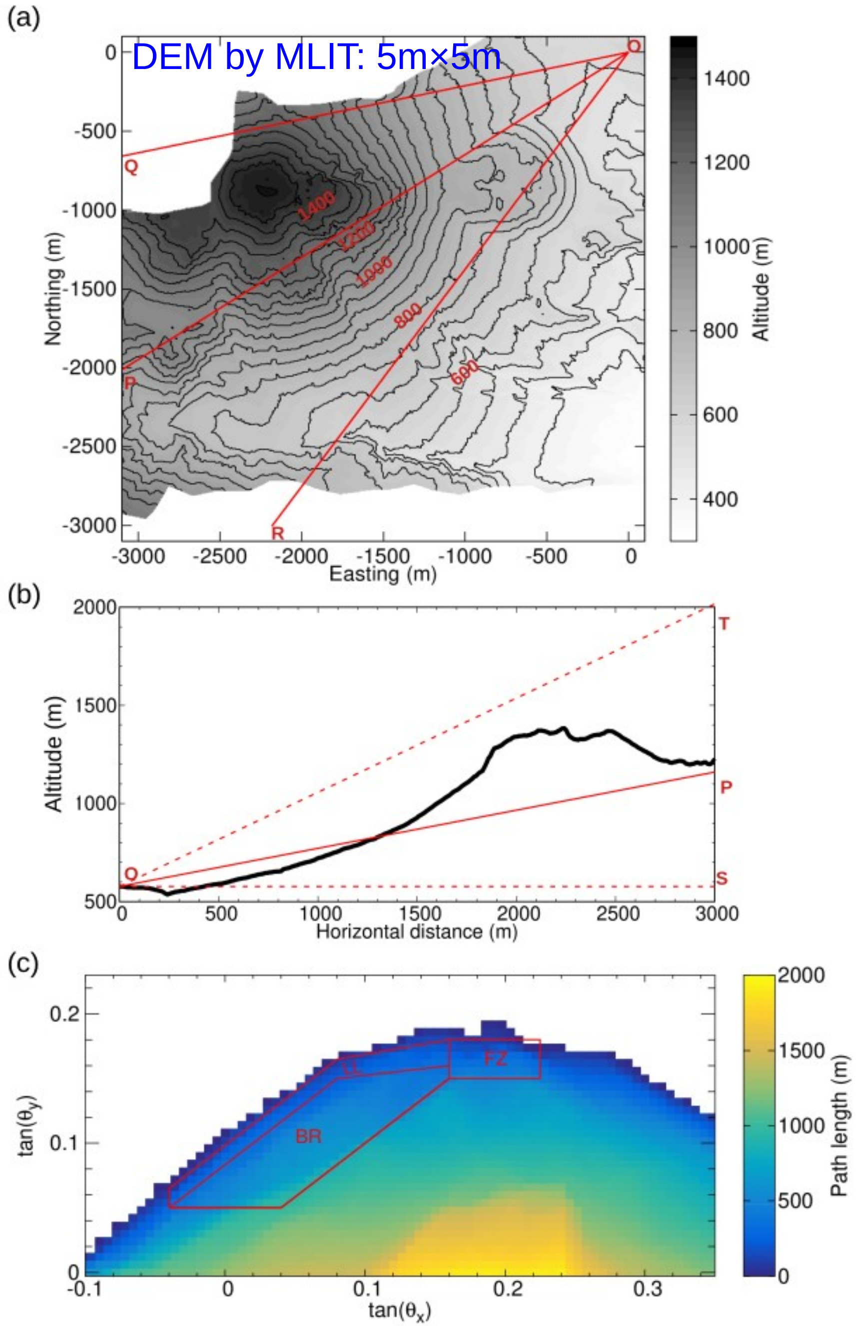

L. Oláh, et al., Geophysical Journal International, 244, ggaf482 (2026) https://doi.org/10.1093/gji/ggaf482

Long-term Weakening of Lava Lobes Inferred from Density Reduction

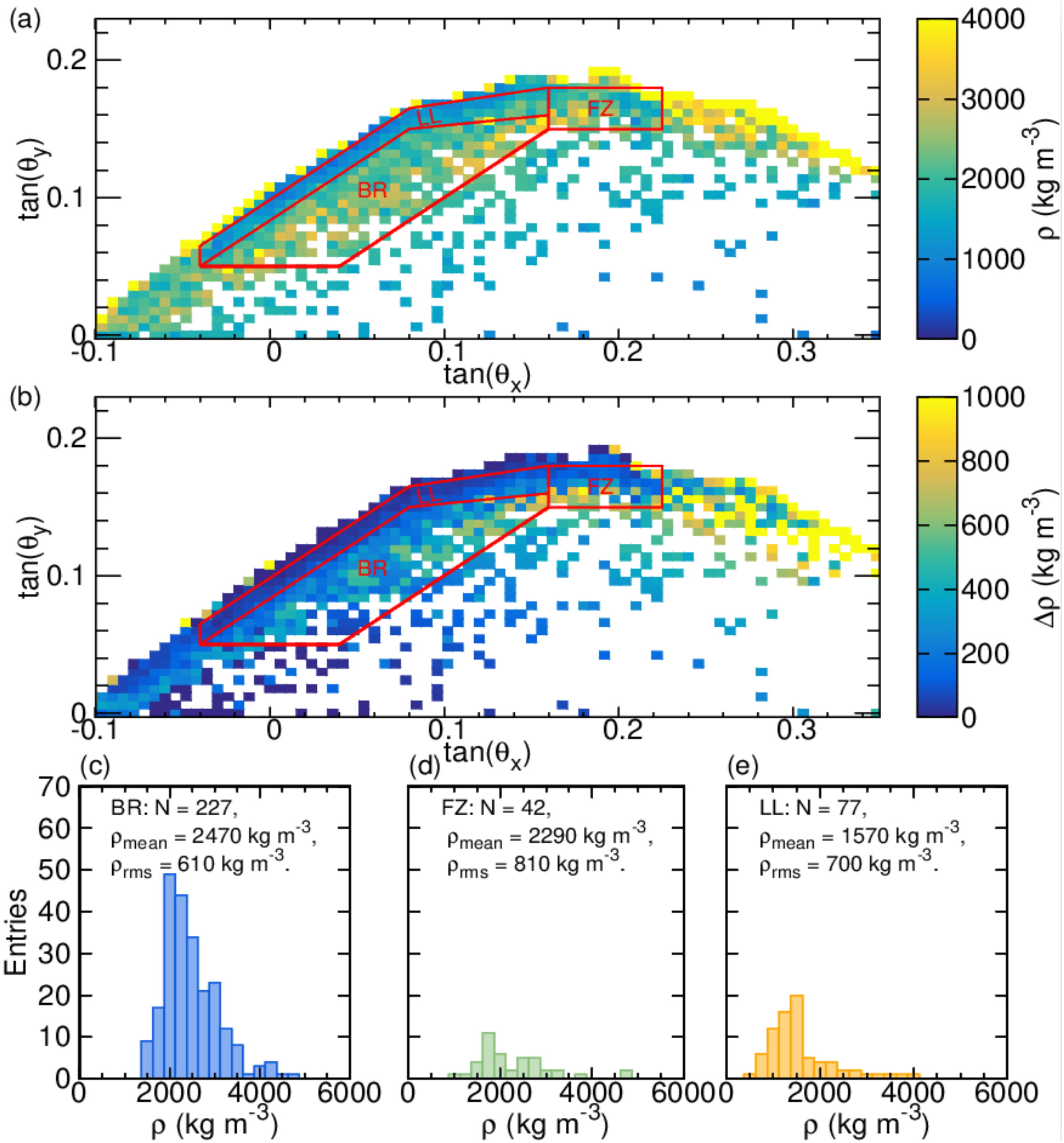

- The obtained high-resolution muographic image shows the **density structure with a spatial resolution of 12 meters.**
- Mean densities were respectively measured as 2470 and 2290 kg m-3 for the **base rock (BR) and a fracture zone (FZ)**, and **both were consistent with the results of prior drilling and sampling experiments.**

Ikeda, R., Kajiwara, T., Omura, K. & Hickman, S., 2008. J. Volc. Geotherm. Res., 175, 13-19. https://doi.org/10.1016/j.jvolgeores.2008.03.036

- The mean density of **lava lobes (LL)** was measured significantly lower value of 1570 kg m−3, **indicating post-eruptive structural weakening.**

Nakada, S., Shimizu, H. & Ohta, K., 1999. J. Volc. Geotherm. Res., 89, 1-22 https://doi.org/10.1016/S0377-0273(98)00118-8

- **Alteration of lava lobes may caused by hydrothermal circulation occurred beneath the lava lobes**

Hashimoto, T. & Tanaka, Y., 1995. Geophys. Res. Lett., 22, 191-194 https://doi.org/10.1029/94GL03077

Saibi, H., Gottsmann, J. & Ehara, S., 2010. J. Volc. Geotherm. Res., 191, 137-147 https://doi.org/10.1016/j.jvolgeores.2010.01.007

L. Oláh, et al., Geophysical Journal International, 244, ggaf482 (2026) https://doi.org/10.1093/gji/ggaf482

Muon Monitoring of Heavy Rainfall Induced Mass Gains in the Lava Lobes

- A comparison between the time-series of muographically measured density-lengths (mean values for period of 7 days) and daily precipitation records suggest that **rainfall-induced gravitational destabilization did not occur during the observational period**.
- When the density-lengths reached their local maxima, those started to decrease within a few days because highly fractured rocks are highly permeable for water. Therefore, the short-term density-length increases had no impact on the stability of the lava lobes during the measurement period.

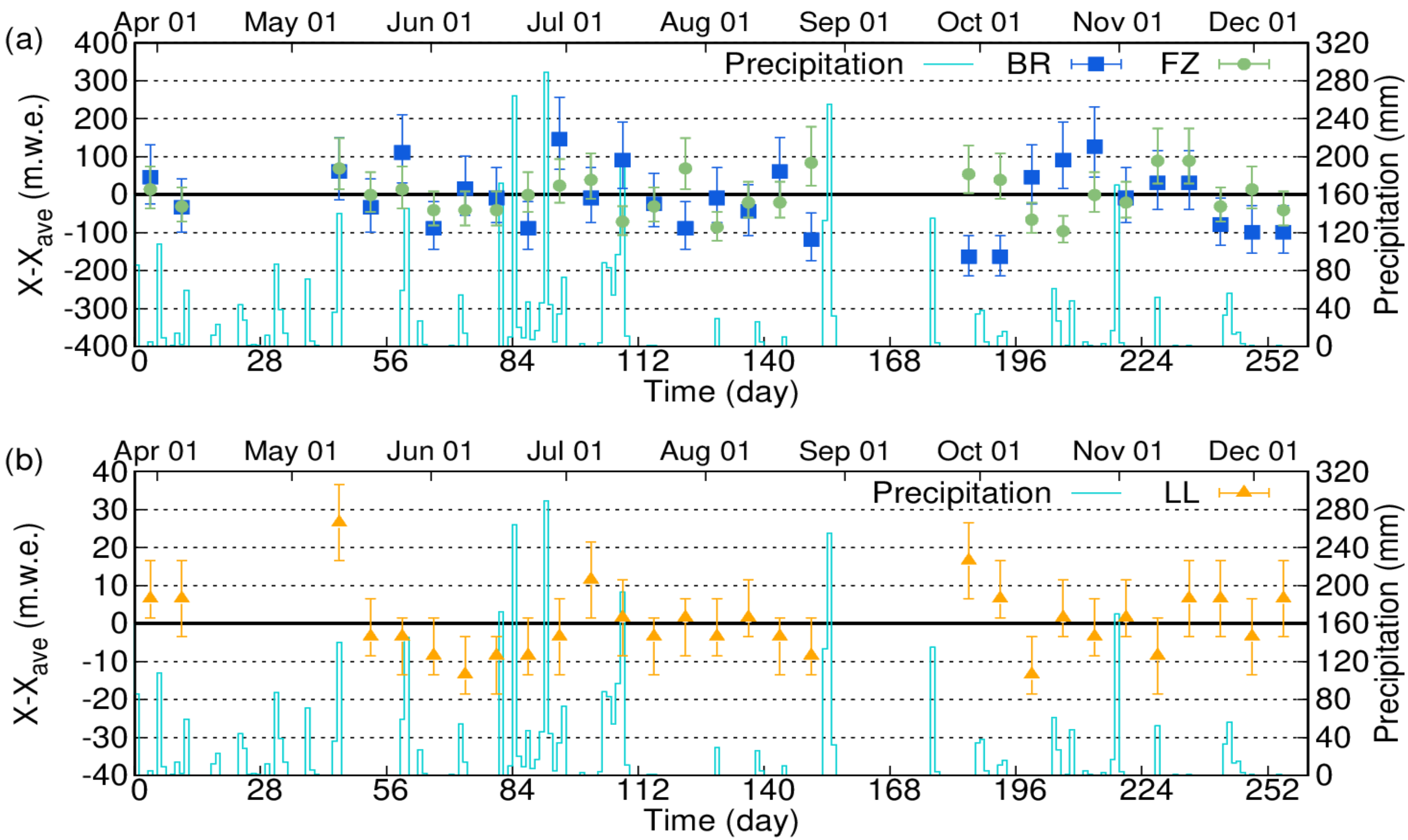

Oláh, L., et al., Geophysical Journal International, 244, ggaf482 (2026) https://doi.org/10.1093/gji/ggaf482

III. First Muography of a Crust-Mantle Transition Zone

- **Oceanic lithosphere (crust, upper solid mantle & Moho** transition zone between them**) cycling:** (1) formation, (2) evolution, (3) desctruction
  → Cycling of matter and energy which produces critical resources, governs natural hazards, and regulates the climate system.
- Only one vertical seismic profile reached seismic layer 2/3 boundary and the **Moho has not yet been reached**
  → **geological nature is not yet well understood**
- Sampling is available but sampling density is low → seismic velocities are different
- **Different seismic layers (layer 2/3 boundary and Moho) are exposed above ground in ophiolites**
  → **Ophiolites help to understand the correlation between oceanic structure and geology**

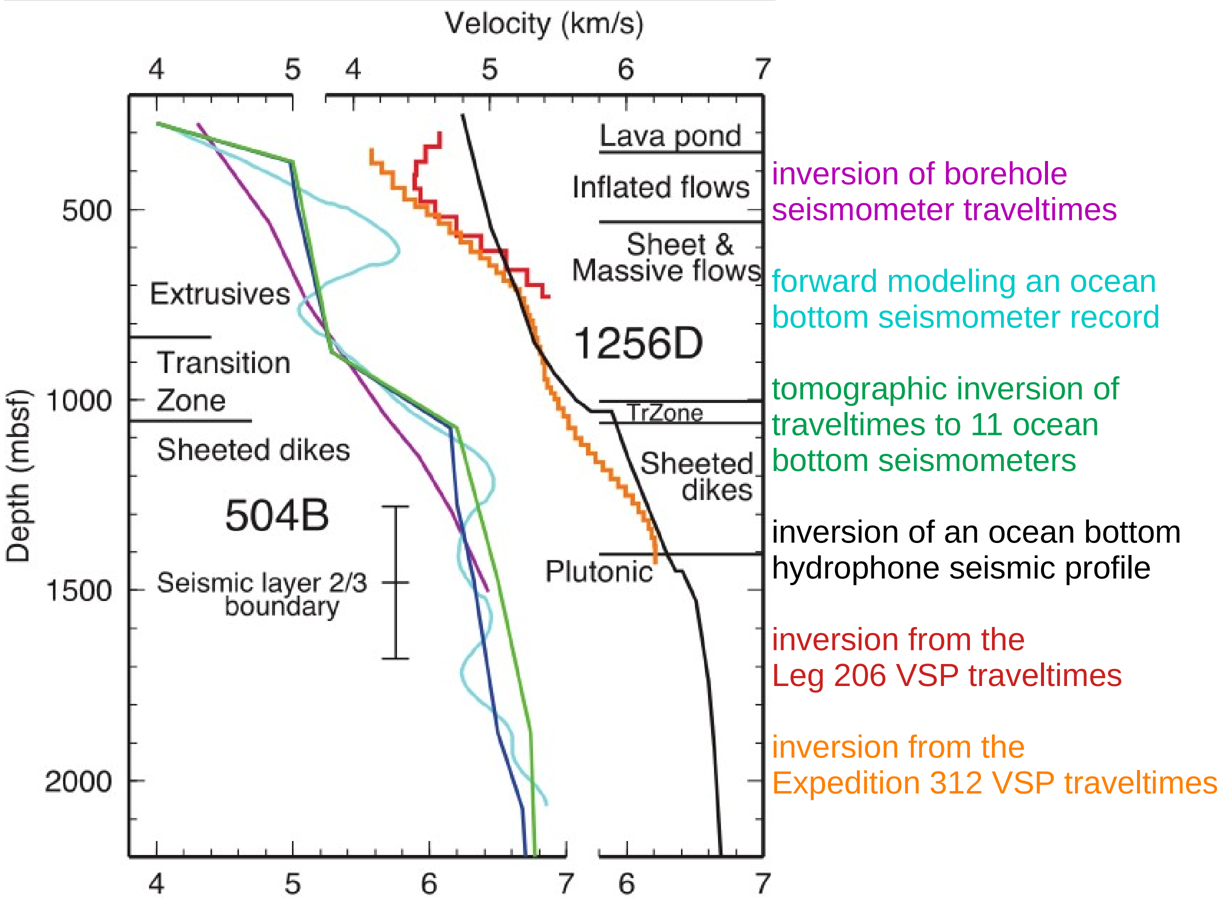

Swift, et al. 2008. Velocity structure of upper ocean crust at Ocean Drilling Program Site 1256. Geochim. Geophys. Geosys., 9, Q10O13, DOI:10.1029/2008GC002188

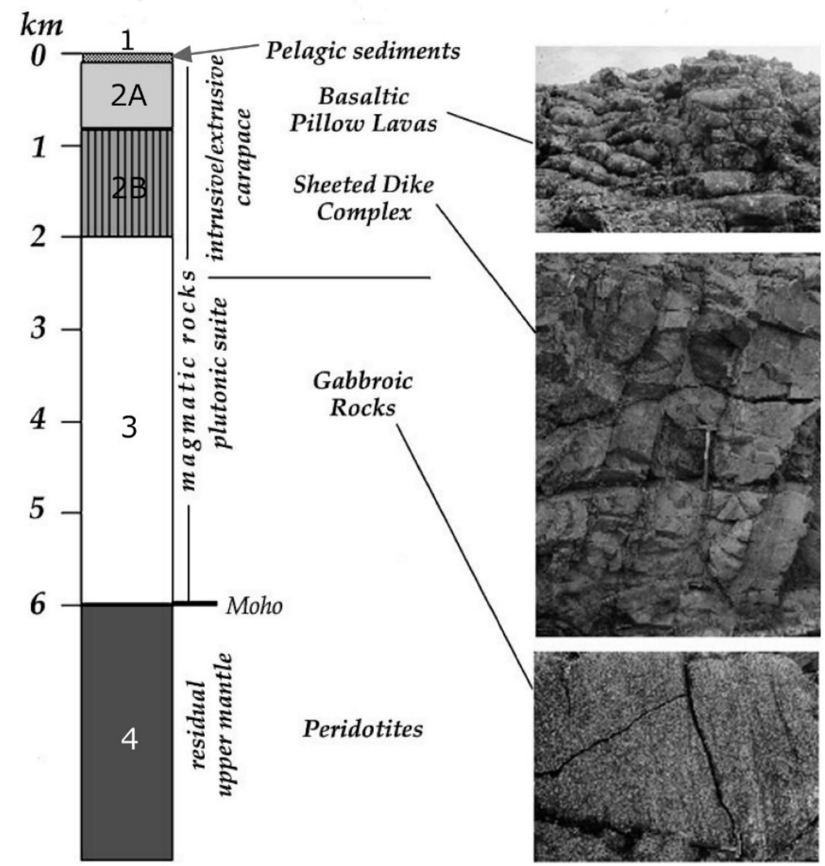

Karson, J.A., Geological structure of the uppermost oceanic crust created at fast- to intermediate-rate spreading centers. *Annu. Rev. Earth Planet. Sci.* **2002**, 30, 347. DOI: 10.1146/annurev.earth.30.091201.141132.

II. The First Experiment at a Moho in Wadi Fizh, Samail-Ophiolite, Sultanate of Oman

Source: Google Maps

Muography can resolve the internal density structure of ophiolites with a spatial resolution of a few meters over large areas, thereby filling the gap between local sampling experiments and large-scale seismic surveys.

L. Oláh, S. Umino, et al. Journal of Advanced Instrumentation in Science, JAIS-499, (2024).
https://doi.org/10.31526/jais.2024.499

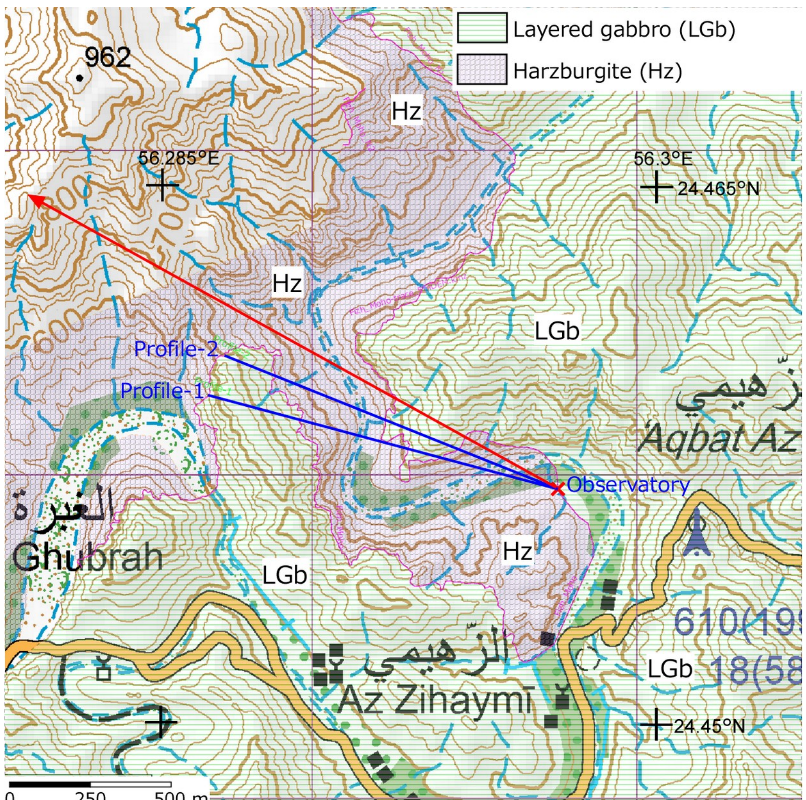

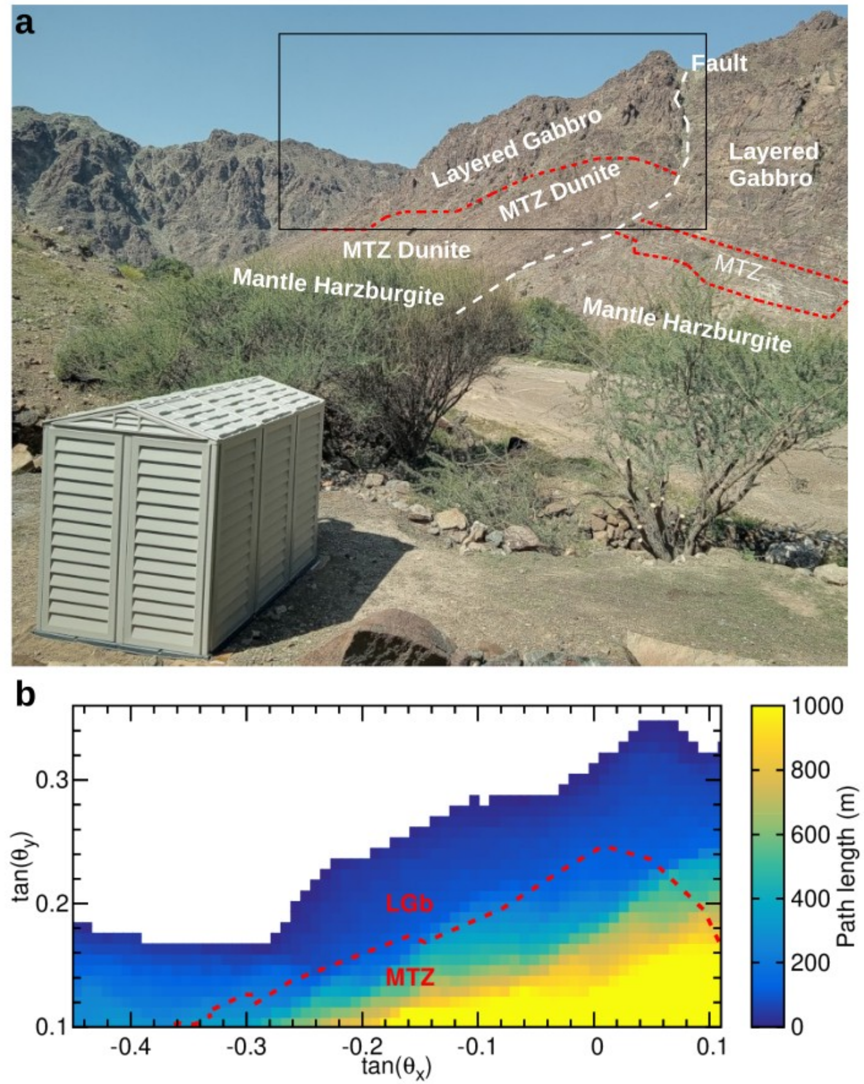

Experimental Setting: Lattitude: 24.45655 deg, Longitude: 56.29703 deg, 298 deg from north **at a distance of 400 m from the Ophiolite**.
Data Collection: A multi-wire-proportional-chamber-based muography system was operated for **171 days**.
L. Oláh, S. Umino, et al. Journal of Geography (Chigaku Zasshi) ,134, 615624, 2025
https://www.jstage.jst.go.jp/article/jgeography/134/6/134_134.615/_article/-char/ja/

Observational Results and Interpretation

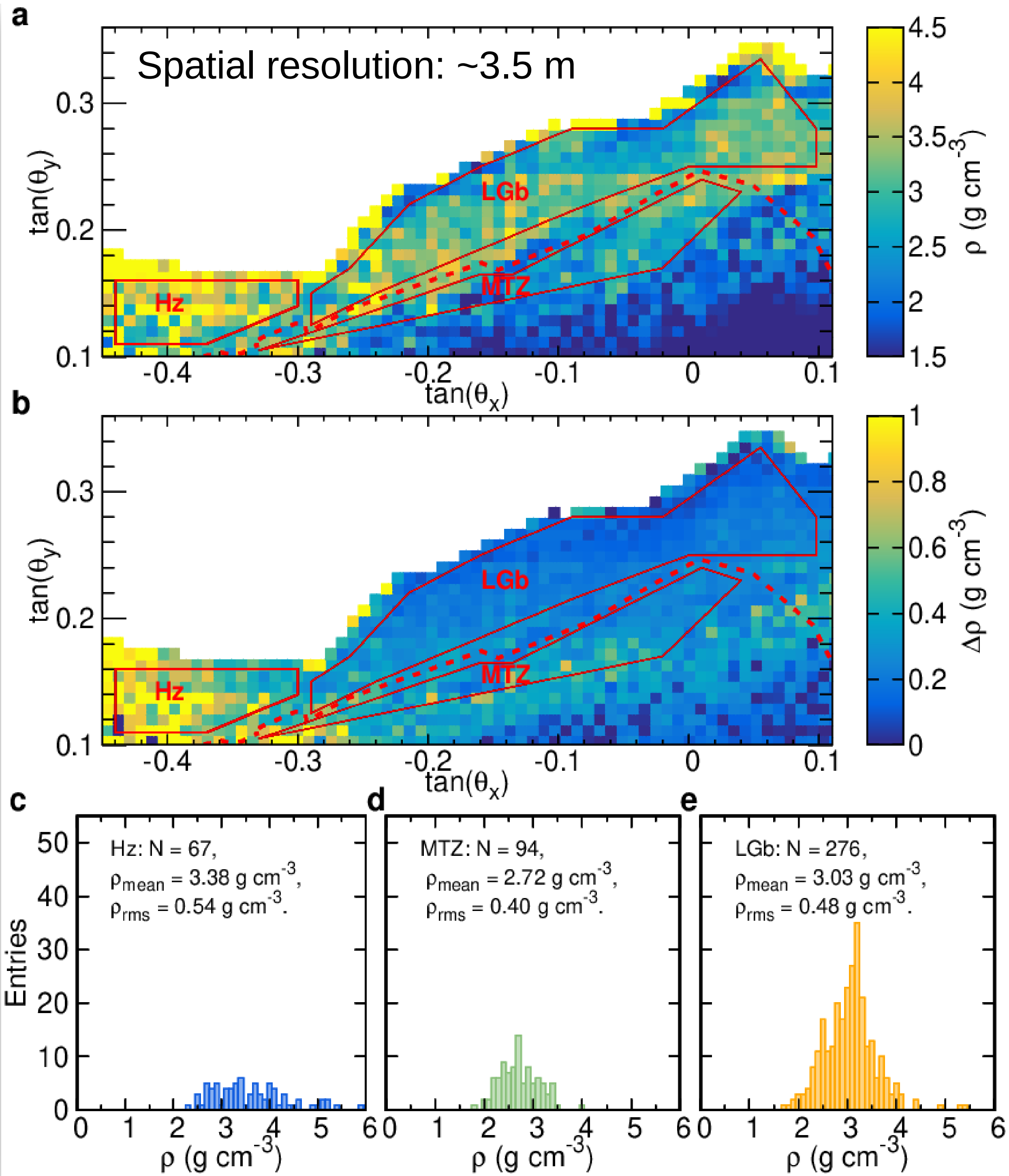

- **The mean density across the LGb** region (3.03 g cm -3) is broadly consistent with reported values for layered gabbros (~2.95-3.0 g cm-3), **suggesting that the layer is relatively intact at meter scales.**

- **The MTZ** exhibits lower mean densities (2.72 g cm -3), which are **compatible with serpentinized dunite and wehrlite as exposed in the field**, although the exact degree of alteration cannot be directly inferred from muography alone.

- High-density anomalies **in the Hz** region (mean 3.38 g cm-3) may indicate **underlying mantle peridotite capped by the thin Lgb layer.**

- **Note:** absolute lithology and fluid–rock interactions cannot be directly determined from muography alone, the technique enables mapping of density contrasts and structural organization at intermediate scales.

L. Oláh et al., First cosmic-ray muography of a crust-mantle transition zone (Under Review at Sci. Rep.)
https://www.researchsquare.com/article/rs-8019975/v1

IV. Summary

- Cosmic-ray muons penetrate hundreds of meters of rock, enabling remote and passive imaging of subsurface density structures and dynamics.
- Muography provides complementary information to conventional geophysical methods, bridging the gap between local sampling and large-scale seismic or satellite observations.
- At Sakurajima, combined muography and satellite deformation measurements revealed magma pathways and shallow magma storage zones controlling eruption activity.

  L. Oláh, et al. Magma migration beneath the active craters of Sakurajima volcano before the 2023 eruption of Showa crater inferred from ground deformation and muon monitoring. Earth Planets Space 77, 196 (2025). https://doi.org/10.1186/s40623-025-02325-3
- At Mount Unzen, muography identified weakened low-density lava lobes, supporting long-term volcanic stability and landslide risk assessment.

  L. Oláh, et al., Geophysical Journal International, 244, ggaf482 (2026) https://doi.org/10.1093/gji/ggaf482
- In the Samail Ophiolite, muography detected density variations and a highly serpentinized Moho, demonstrating its value as a complementary tool for imaging crust–mantle architecture and Earth subsurface structures.

  L. Oláh et al., First cosmic-ray muography of a crust-mantle transition zone (Under Review at Sci. Rep.) https://www.researchsquare.com/article/rs-8019975/v1